ISBN: 978-3-95450-225-7 ISSN: 2673-5571 doi:10.18429/JACoW-HB2021-MOAC3

DEVELOPMENT OF AN INJECTION-PAINTED SELF-CONSISTENT BEAM IN THE SPALLATION NEUTRON SOURCE RING

A. Hoover, University of Tennessee, Knoxville, U.S.A.
N. J. Evans*, T. Gorlov, J. Holmes, Oak Ridge National Laboratory, Oak Ridge, U.S.A.

Abstract

A self-consistent beam maintains linear space charge forces under any linear transport, even with the inclusion of space charge in the dynamics. Simulation indicates that it is possible to approximate certain self-consistent distributions in a ring with the use of phase space painting. We focus on the so-called Danilov distribution, which is a uniform density, rotating, elliptical distribution in the transverse plane and a coasting beam in the longitudinal plane. Painting the beam requires measurement and control of the orbit at the injection point, and measuring the beam requires reconstruction of the four-dimensional (4D) transverse phase space. We discuss efforts to meet these requirements in the Spallation Neutron Source (SNS) ring.

INTRODUCTION

We define a self-consistent beam as one that maintains linear space charge forces under any linear transport, even with the inclusion of space charge in the dynamics. Several desirable properties stem from the linearity of the space charge force: the emittance is conserved, the space charge tune shift is minimized, and the space charge tune spread is eliminated. An ongoing project is to determine whether a self-consistent beam can be approximated in reality.

Various self-consistent distributions were derived in [1]; of particular interest for our purposes is the so-called Danilov distribution, which is a uniform density ellipse in the transverse plane and a coasting beam in the longitudinal plane. Particles in the distribution occupy elliptical modes so that the four-dimensional (4D) transverse emittance vanishes. Equivalently, one of the intrinsic emittances $\varepsilon_{1,2}$ vanishes depending on the sign of the angular momentum [2]. The intrinsic emittances are conserved even with space charge, but the apparent emittances $\varepsilon_{x,y}$ are not [3].

In the linear approximation, it is possible to create an approximate Danilov distribution in a circular machine using phase space painting. This can be done by moving the injection coordinates along an eigenvector of the ring transfer matrix with square root time-dependence. In other words,

$$\mathbf{x}(t) = \sqrt{2J}\, Re\left\{\mathbf{v}e^{-i\mu}\right\}\sqrt{t}, \tag{1}$$

where $\mathbf{x} = (x, x', y, y')$ is the phase space location of the injection beam in the frame of the circulating beam, J is an amplitude, μ is a phase, $\mathbf{v}$ is an eigenvector of the ring transfer matrix, and t is a time variable normalized to the range [0, 1]. We call this *elliptical painting*. The turn-by-turn projection of the eigenvector onto any 2D subspace

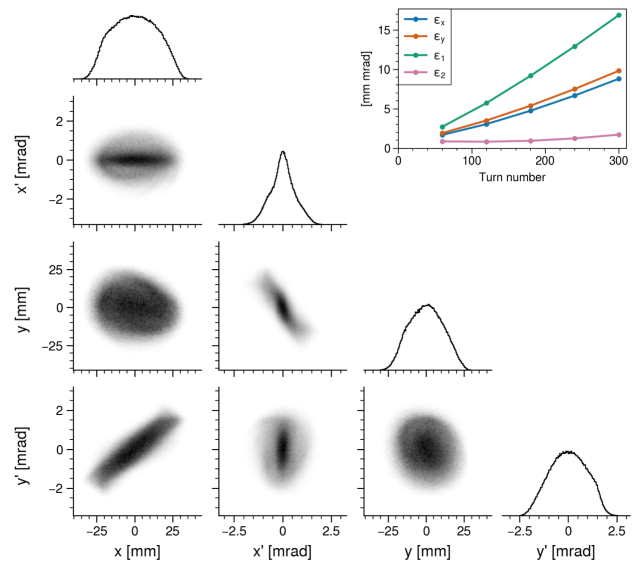

Figure 1: ORBIT simulation of elliptical painting in the SNS ring. Bottom left: 2D projections of the final 4D phase space distribution. Top right: emittance growth during injection.

of the 4D phase space will trace an ellipse, and the square root time-dependence ensures the uniform density of the projected distributions at all times. Since the particles lie along an eigenvector, the intrinsic emittance associated with the other eigenvector will be zero. We note that performing this method in an uncoupled lattice results in a flat beam ($\varepsilon_x = 0$ or $\varepsilon_y = 0$) unless the horizontal and vertical tunes are equal.

Simulations suggest that the various conditions required for elliptical painting to produce a self-consistent beam will approximately hold in the Spallation Neutron Source (SNS) [4]. Figure 1 shows the results of one such simulation. The core of the final 1D projections resemble those of ideal elliptical projections, and it can also be seen from the linear emittance growth and constant/small ε_2 that the beam remains reasonably close to a Danilov distribution during injection.

Several steps were necessary to achieve this simulated result. First, the painting path was chosen to follow a line in the x-y' plane. Deviation from this path was found to increase beam losses due to machine specifics. Additional motivation for x-y' painting comes from study of the beam envelope equations in [3]. The beam tilts throughout the ring, but the matched solution with space charge is upright at locations where $\alpha \approx 0$ such as the injection point. A tilted beam at

* evansnj@ornl.gov

ISBN: 978-3-95450-225-7 ISSN: 2673-5571 doi:10.18429/JACoW-HB2021-MOAC3

these locations leads to severe mismatch oscillations due to linear coupling from space charge. Second, the apparent emittances were kept nearly equal, again in consideration of the matched beam. Third, the ring RF cavity voltages were decreased to better approximate a coasting beam. Fourth, the beam energy was lowered to 0.6 GeV to increase the effective kicker strength; the number of injected turns was decreased to 300 to compensate for the resulting increase in space charge strength. Fifth, orbit corrector dipoles in the injection region were used to assist the vertical kickers. With these settings, a maximum vertical slope of 1.7 mrad was reached. Finally, a solenoid magnet was added to the ring to mitigate the effect of fringe fields near the difference resonance $\nu_x - \nu_y = 0$ by splitting the eigentunes of the ring transfer matrix.

In the rest of this paper, we report on the development of tools at the SNS to (a) measure and control the orbit in the injection region and (b) measure the 4D phase space of the painted beam. We then present initial experimental results.

RING INJECTION CONTROL

The closed orbit in the injection region is controlled by varying the current in eight independent dipole kicker magnets — four in each plane. Each magnet is given a square root waveform; what remains is to determine the initial/final voltages to produce the desired phase space coordinates at the injection point. An OpenXAL application was developed to this end [5].

The positions and angles at the injection point are estimated in the following way. A single minipulse from the linac is injected and stored in the ring with the kicker magnets at a constant voltage and a turn-by-turn signal is collected from a beam-position-monitor (BPM) in the ring. The average signal over multiple minipulses is fit with a Gaussian-damped sinusoid of the form [6]:

$$x(t) = A_0 + Ae^{kt^2} \cos(\mu + \mu_0), \tag{2}$$

where t is the turn number. The parameter A gives the betatron amplitude, $\mu/2\pi$ gives the fractional tune, and μ_0 gives the particle phase at the BPM. The phase space coordinates at the injection point are recovered by combining these parameters with the linear ring model. This is repeated for each BPM to give an estimated mean and standard deviation of the phase space coordinates at the injection point. An example fit is shown in Fig. 2.

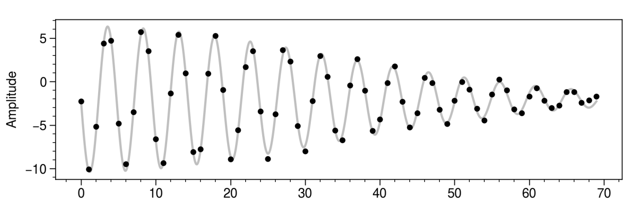

Figure 2: Turn-by-turn BPM signal fit with Eq. (2).

The next issue is how to control the phase space coordinates at the injection point. Each kicker magnet is calibrated by applying a voltage difference to the magnet and measuring the orbit response using the ring BPMs; the angular kick associated with the magnet is varied until the model orbit agrees with the measured orbit. It was also found that slight quadrupole corrections are necessary for the model to agree with measurements. The standard deviation of the measured phase space coordinates is small after this calibration. One can then ask the model for a change in coordinates, update the kickers accordingly, and measure the new coordinates, iterating if necessary.

The kicker magnets have limited strengths and are unipolar, which limits the minimum distance from the and the maximum angle at the injection point. In fact, the closed orbit cannot reach the foil at production energy (1 GeV). As mentioned previously, the beam energy can be lowered to increase the effective kicker strength; however, this is a significant task for SNS operators due to issues related to the SNS timing system. Attempts to lower to 0.6 GeV were unsuccessful, but an energy of 0.8 GeV was recently achieved. The use of orbit corrector dipoles to assist the kickers is complicated by the fact that the correctors are turned on during production, so their variation leads to significant closed-orbit waves throughout the ring. The use of orbit correctors is left as a future optimization.

FOUR-DIMENSIONAL PHASE SPACE MEASUREMENT

Determining how closely a painted beam resembles a Danilov distribution requires measurement of the 4D transverse phase space distribution. A direct measurement such as a slit-scan is not possible, so the phase space distribution must be reconstructed from lower-dimensional projections.

Reconstruction from 1D Projections

The transverse covariance matrix can be reconstructed 1D projections by estimating the $\langle xx \rangle$, $\langle yy \rangle$, and $\langle xy \rangle$ moments at four or more locations or optics settings [7,8]. Four reliable wire-scanners are available to perform this measurement in the ring-target beam transport (RTBT) section of the SNS, just before the target, each equipped with a horizontal, vertical, and diagonal wire. The wire-scanners can be run in parallel in approximately five minutes. The optics in the RTBT can be changed, but there are several constraints. First, the β functions must be kept reasonably small throughout the RTBT to minimize beam loss. Second, the beta functions at the target must be kept at their nominal values. Third, control of the optics *between* the wire-scanners is limited by the fact that two power supplies control the eight quadrupoles in the measurement region.

We tested the method on a production beam by scanning the phase advances at WS24 (the last wire-scanner in the group) in a 30-degree window over ten steps. At each step, the two power supplies (eight quadrupoles) upstream of WS24 were varied to obtain the correct phase advances, then

ISBN: 978-3-95450-225-7 ISSN: 2673-5571 doi:10.18429/JACoW-HB2021-MOAC3

five quadrupoles downstream of WS24 were varied to reset the β functions at the target. The results are shown in Fig. 3. The colored lines are defined by $x = \sqrt{\langle xx \rangle}$ at the wire-scanners transported back to the reconstruction location. The coordinates are normalized by the reconstructed Twiss parameters.

Errors can appear in the transfer matrix elements or measured moments. Errors in the measured moments are expected to be small since there is very little bunch-to-bunch variation in the profiles, while the correlation between x and y could have a larger error since it is calculated indirectly. Errors in the transfer matrix are also expected to be small since the reconstruction location is close to the wire-scanners. We use the standard deviations of the ten reconstructed moments obtained from the linear least squares estimator in our analysis and propagate these to obtain the uncertainties in the beam parameters [9]. The reconstructed Twiss parameters are close to the model parameters computed from the linear transfer matrices of the ring and RTBT. The intrinsic emittances are almost equal to the apparent emittances, showing that there is very little cross-plane correlation in the beam.

We found that two measurements (eight profiles) produced nearly the same values and uncertainties as the entire scan, but that the reconstruction failed when using only one measurement (four profiles), producing imaginary intrinsic emittances. This is a known problem; certain optics between wire-scanners lead to an ill-conditioned system of equations [10]. To solve this problem, we varied the phase advances at WS24 and recorded the number of failed fits from a Monte Carlo simulation at each setting. This revealed

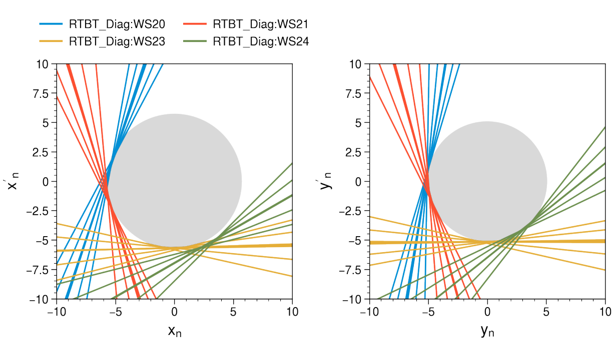

Parameter	Measurement	Model
β_x [m/rad]	22.06 ± 0.29	22.00
β_y [m/rad]	4.01 ± 0.02	3.81
α_x [rad]	2.33 ± 0.04	2.37
α_y [rad]	-0.49 ± 0.01	-0.60
ε_1 [mm mrad]	33.02 ± 0.05	-
ε_2 [mm mrad]	25.67 ± 1.03	-
ε_x [mm mrad]	32.85 ± 0.05	-
ε_y [mm mrad]	25.87 ± 0.12	-

Figure 3: Reconstructed beam parameters and graphical output from the multi-optics emittance measurement of a production beam.

that the measurement sensitivity can be made tolerable by changing the horizontal(vertical) phase advance at WS24 by 45(-45) degrees.

Reconstruction from 2D Profiles

The SNS target nose is prepared with a luminescent Cr:Al2O3 coating that allows imaging of the beam distribution on the target [11]. The target imaging system is immediately useful for our purposes to verify the shape, density, and tilt of the painted beam, especially relative to a production beam. It is also possible to vary the phase advances from a point upstream of the target to the target, which effectively shows a 2D projection of the distribution at different "angles" in 4D phase space. Tomographic methods could be employed to reconstruct the 4D phase space distribution using these 2D projections [12]. We are currently determining the feasibility of this approach.

INITIAL RESULTS

We first discuss the 4D phase space measurement of a production beam for later comparison. The SNS operates at 1 GeV during neutron production and employs correlated painting with an initial offset of the closed orbit from the foil [13]. We used the same painting waveforms but decreased the painting time so that only 500 minipulses are injected in instead of 1000; i.e., the final beam is the same size but half the intensity. We are free to extract and measure the beam at any point during injection; we chose to collect measurements every 50 turns.

The wire-scanner measurements and reconstructed emittances are displayed in Fig. 4. The initial orbit offset from the foil is evident in the hollow wire-scanner profiles. The reconstructed emittances indicate very small cross-plane correlation throughout injection. Since in these cases the cross-plane moments are solved for exactly using four wire-scanners, we cannot use the uncertainty estimate from linear least squares for the intrinsic emittances; instead, we use the worst case from Fig. 3 of approximately 4% uncertainty.

We now discuss our first attempt at elliptical painting. The beam energy was lowered to 0.8 GeV to reach the closed orbit to the foil, and the ring tunes were then set equal at 6.18. With these machine settings, a maximum vertical slope of 1.1 mrad was attained, and we chose to paint to a maximum horizontal position of 20 mm over 500 turns. The bunch length was set to approximately half of the ring length, and the ring RF cavities were left untouched. The measurement from Fig. 4 was then repeated. The results are displayed in Fig. 5.

The measured apparent emittances increase linearly from near zero as intended, and the wire-scanner profiles are no longer hollow. There is a small amount of cross-plane correlation present during injection, but the 4D emittance is not close to zero. The wire-scanner profiles are also somewhat peaked as opposed to the elliptical profiles that would be present in a uniform density elliptical beam. The measured Twiss parameters are not the same as the model Twiss pa-

ISBN: 978-3-95450-225-7 ISSN: 2673-5571 doi:10.18429/JACoW-HB2021-MOAC3

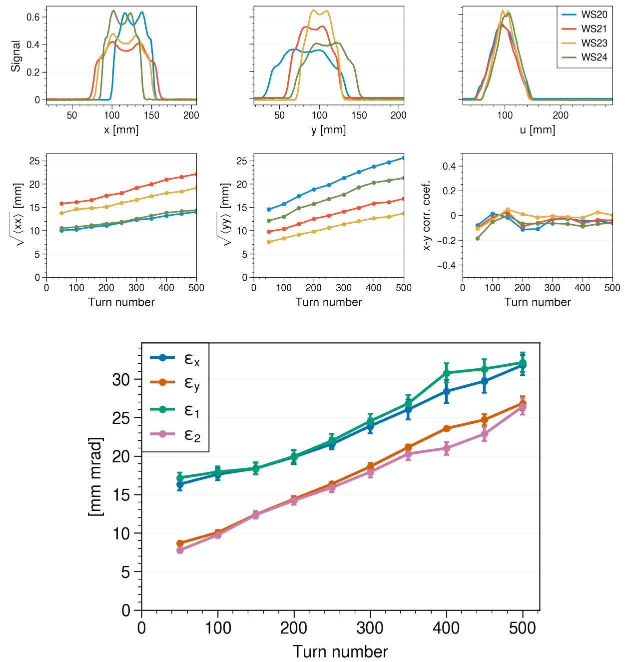

Figure 4: Measured beam during correlated painting. Top: measured wire-scanner profiles after injection. Middle: measured beam moments during injection. Bottom: reconstructed emittances during injection.

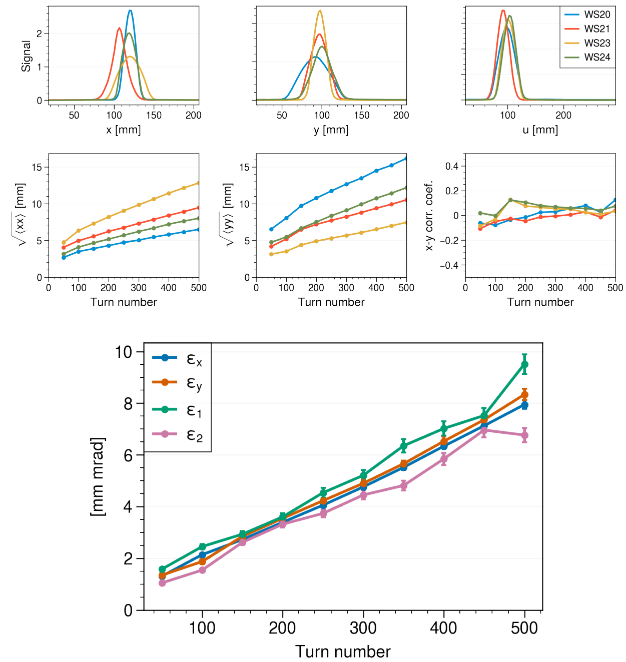

Figure 5: Measured beam during elliptical painting. Top: measured wire-scanner profiles after injection. Middle: measured beam moments during injection. Bottom: reconstructed emittances during injection.

rameters; this is expected for higher space charge since the beam Twiss parameters will adjust to the matched solution with space charge in the ring.

The left column of Fig. 6 shows a simulation of this case using PyORBIT [14]. The cross-plane correlation is largely eliminated by fringe fields early on; however, the intrinsic emittances split around turn 100 and remain significantly different than the apparent emittances for the rest of injection. It is known from previous studies that the space charge force in an elliptical beam has a stabilizing effect similar to solenoid fields. Although blurred, the x-y' projection of the distribution has a higher density along the painting path. The reason for the disagreement between this simulation and our measurements is under investigation.

Several modifications could bring the painted beam closer to a self-consistent state. The first is to decrease the space charge strength by increasing the painted emittances and/or decreasing the beam intensity. It is evident from the simulated emittance growth in the second half of injection that the space charge effect on the beam is quite strong. There is no limit on the horizontal emittance since it is increased by lowering the kicker voltages, but the vertical emittance is fixed unless the orbit corrector dipoles provide additional help. Although it is undesirable to greatly separate the horizontal and vertical emittances, simulation indicates that increasing x_{max} from 21 mm to 31 mm has a positive effect. As seen in the right column of Fig. 6, ε_2 remains nearly constant during the second half of injection, and the final x-y' projection is clustered along the painting path. A second possible improvement is to insert a solenoid magnet in the ring to mitigate fringe field effects; this is planned to occur in early 2022. A third possibility is to modify the ring RF voltages and bunch length to better approximate a coasting beam.

CONCLUSION

Several issues have been resolved in our project to create an approximately self-consistent beam in the SNS ring. First, an application has been developed to measure and control the closed orbit at the injection point. Second, a method to reconstruct the transverse covariance matrix from 1D projections has been implemented and the optics have been modified to minimize the measurement time. Third, the SNS energy has been lowered to inject particles directly onto the closed orbit. Elliptical painting has been carried out and compared with simulation and with correlated painting. Although the resulting beam is distinguishable from a normal production beam, it does not exhibit the desired relationships between the phase space coordinates; however, modifications to both the lattice and painting parameters have the potential to provide a significant improvement in future experiments.

REFERENCES

[1] V. Danilov, S. Cousineau, S. Henderson, and J. Holmes, "Self-consistent time dependent two dimensional and three dimensional space charge distributions with linear force", *Phys. Rev. Accel. Beams*, vol 6, p. 094202, 2003. doi: 10.1103/PhysRevSTAB.6.094202

ISBN: 978-3-95450-225-7 ISSN: 2673-5571 doi:10.18429/JACoW-HB2021-MOAC3

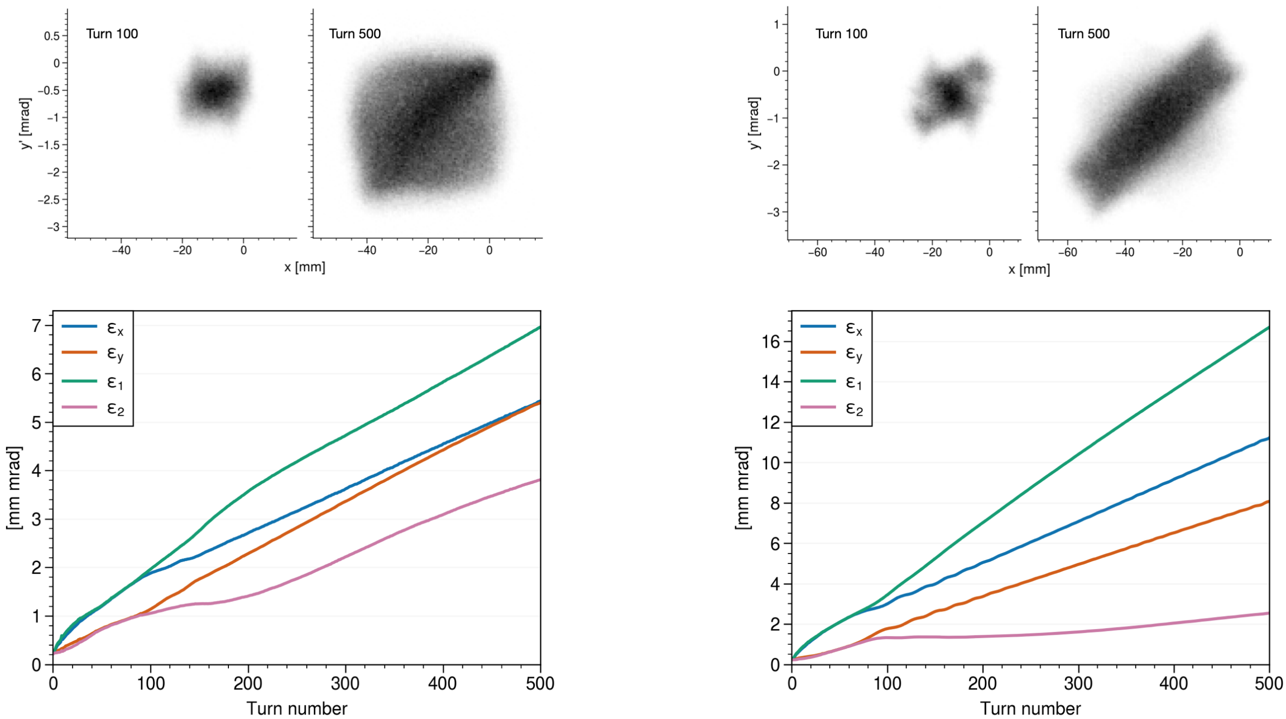

Figure 6: PyORBIT simulation of elliptical painting in the SNS ring without solenoids. In both columns, y'_{max} = 1.1 mrad. In the left column, x_{max} = 21 mm, while in the right column, x_{max} = 31 mm. The lower plots show the emittance growth during injection, while the upper plots show the x-y' projections at turn 100 and 500.

[2] L. Groening, C. Xiao, and M. Chung, "Particle beam eigen-emittances, phase integral, vorticity, and rotations", *Phys. Rev. Accel. Beams*, vol. 24, p. 054201, 2021. doi:10.1103/PhysRevAccelBeams.24.054201

[3] A. Hoover, N. J. Evans, and J. A. Holmes, "Computation of the matched envelope of the Danilov distribution", *Phys. Rev. Accel. Beams*, vol. 24, p. 044201, 2021. doi:10.1103/PhysRevAccelBeams.24.044201

[4] J. A. Holmes, T. Gorlov, N. J. Evans, M. Plum, and S. Cousineau, "Injection of a self-consistent beam with linear space charge force into a ring", *Phys. Rev. Accel. Beams*, vol. 21, p. 124403, 2018. doi:10.1103/PhysRevAccelBeams.21.124403

[5] N. Milas *et al.*, "Open XAL Status Report 2021", in *Proc. IPAC'21*, Campinas, Brazil, May 2021, pp. 3421–3423. doi:10.18429/JACoW-IPAC2021-WEPAB319

[6] T. Pelaia, "Parameter Estimation of Gaussian-Damped Sinusoids from a Geometric Perspective", http://arxiv.org/abs/1604.05167/, 2021.

[7] E. Prat and M. Aiba, "Four-dimensional transverse beam matrix measurement using the multiple-quadrupole scan technique", *Phys. Rev. Accel. Beams*, vol. 17, p. 052801, 2014. doi:10.1103/PhysRevSTAB.17.052801

[8] "Measurement and Correction of Cross-Plane Coupling in Transport Lines", in *Proc. LINAC'00*, Monterey, CA, USA, Aug. 2000, paper MOC19, pp. 196–198.

[9] A. Faus-Golfe, J. Navarro, N. Fuster Martinez, J. Resta Lopez, and J. Giner Navarro, "Emittance reconstruction from measured beam sizes in ATF2 and perspectives for ILC", *Nucl. Instrum. Methods Phys. Res. A*, vol. 819, pp. 122-138, 2016. doi:10.1016/j.nima.2016.02.064

[10] I. Agapov, G. A. Blair, and M. Woodley, "Beam emittance measurement with laser wire scanners in the International Linear Collider beam delivery system", *Phys. Rev. Accel. Beams*, vol. 10, p. 112801, 2007. doi:10.1103/PhysRevSTAB.10.112801

[11] W. Blokland, T. McManamy, and T. J. Shea, "SNS Target Imaging System Software and Analysis", in *Proc. BIW'10*, Santa Fe, NM, USA, May 2010, paper TUPSM003, pp. 93–97.

[12] K. M. Hock and A. Wolski, "Tomographic reconstruction of the full 4D transverse phase space", *Nucl. Instrum. Methods Phys. Res. A*, vol. 726, pp. 8–16. 2013. doi:10.1016/j.nima.2013.05.004

[13] S. Henderson *et. al.*, "The Spallation Neutron Source accelerator system design", *Nucl. Instrum. Methods Phys. Res. A*, vol. 763, pp. 610-673, 2014. doi:10.1016/j.nima.2014.03.067

[14] A. Shishlo, S. Cousineau J. Holmes, and T. Gorlov, "The Particle Accelerator Simulation Code PyORBIT", *Procedia Comput. Sci.*, vol. 51, p. 1272, 2015. doi:10.1016/j.procs.2015.05.312